Reprinted from ANALYTICAL AND QUANTITATIVE CYTOLOGY AND HISTOLOGY
Vol. 22 No. 2, April 2000

Topologic Distribution of Different Types of Neurons in the Human Putamen

Oliver Schmitt, M.D., **Reinhard Eggers,** M.D., and **Herbert Haug,** M.D.

OBJECTIVE: To test the assumption that the various types of neuron in the human putamen appear to be randomly distributed and to quantify the way in which they are arranged, stochastic geometry, multivariate analysis and the interactive evaluation technique were employed.
STUDY DESIGN: Twenty-seven human putamina without demonstrable signs of neurologic change were dissected out, fixed in 4% formalin and embedded in paraffin. The 20-µm paraffin sections were stained in an aldehyde-fuchsin and cresyl-violet solution, which makes it possible to distinguish between seven different neuron populations in the putamen. The gravity centers, size and form factors of these neurons were determined morphometrically under a light microscope. The data obtained were used to calculate the spatial distribution of the neurons by interactive and structure analytical methods.
RESULTS: Visual point field analysis revealed an irregular arrangement of the different types of neurons. Point process analysis detected a significant hard core process of type 1 and a cluster process of type 6 neurons. With nearest neighborhood analysis, significant differences were found between certain populations of neurons and Poisson processes. Comparison of the results of multivariate cluster analysis with the investigator-dependent results of visual point field analysis showed clear differences.
CONCLUSION: By means of structure analytical methods, the arrangement of different populations of neurons can be demonstrated. Some neuronal distributions are detectable only by using one of these techniques. The question of random or nonrandom distribution of the neurons in the human putamen can now be answered definitively: arrangement of the different populations of neurons is structured. (Analyt Quant Cytol Histol 2000;22:155–167)

Keywords: neurons, putamen, multivariate analysis, stochastic processes, cluster analysis.

The debate about the spatial distribution of the different types of neurons in the human putamen was initiated by Spiegel.[33] It has since been continued by Vogt and Vogt,[37] Foix et al,[8] Kemp,[21] Fox et al,[9] Kemp et al,[20] Tennyson et al,[35] Böttcher et al[3] and Lu et al[22] and possibly brought to a satisfactory conclusion by Graybiel and Ragsdale[12] with their concept of striosomes and matrisomes.[18] The quantitative and qualitative results of cresyl-violet staining, silver impregnation, enzyme histochemistry and immunohistochemistry represent the outcome of a large number of cytoarchitectural methods of investigating the arrangement of the neurons. All those methods have one thing in common: they do

From the Department of Anatomy, Medical University of Lübeck, Lübeck, Germany.
Drs. Schmitt and Eggers are Scientists.
Dr. Haug is Senior Scientist.
Address reprint requests to: Oliver Schmitt, M.D., Department of Anatomy, Medical University of Lübeck, Ratzeburger Allee 160, D-23538 Lübeck, Germany (schmitt@anat.mu-luebeck.de).

Financial Disclosure: The authors have no connection to any companies or products mentioned in this article.
Received for publication February 17, 1998.
Accepted for publication July 20, 1999.

0884-6812/00/2202-0155/$15.00/0

not depend upon quantification of spatial arrangement. However, the structural parameters *between* cells have been systematically determined[2,5,23,27,28] because a prerequisite of the proper functioning of any neuronal system is its correct structural organization. The precise position of neurons in space, their processes and their connecting synapses is essential if they are to function systematically.[1,13,29]

We have summarized all the methods used for investigating the structure and spatial relationship between distinguishable objects under the term *structure analysis*.[30,31] This is meaningful with regard to methodologic classification since modified and self-developed techniques, stochastic geometry and multivariate analysis have been used.

The aim of this study was to determine the spatial distribution of each type of neuron in the normal human putamen by means of various analytical procedures. This is important because of the functional implications of the structure and distribution of those neurons that make up the various complex networks. The application of multivariate methods to the distribution of neurons in the human putamen is reported below for the first time. The investigation of these techniques was necessary in order to compare the classifications of fuzzy neuronal distribution patterns arrived at interactively by investigators using various types of automated classification. All the methods described below are embedded in a consistent theoretical framework. Their application to such unique data sets has not been reported before.

The formal structure, application and results of the different structure analytical procedures can be compared within large samples. Finally, this framework and its application to the present investigation are explained in detail.

Materials and Methods

The investigation was based on 27 human putamina from subjects without any signs of neurologic disease and with a uniform age distribution (25–100 years; $\bar{x} = 57.5$). The brains were fixed in 4% formalin diluted with a 0.9% sodium chloride solution. Embedding was carried out as described by Haug.[16] Histologic sections, 20 μm, were cut and mounted on gelatinized slides.

In order to distinguish between the types of neurons in the putamen, each section was stained in an aldehyde-fuchsin and cresyl-violet (AFC) solution.[4,31] AFC stain has a high affinity for neurolipofuscins. The cytoplasm of the neurons is stained by the cresyl-violet component. The result is a richly contrasted and detailed section that permits classification of seven morphologically different types of neurons. In the terminology of Graveland et al,[11] type 1 and 2 neurons are comparable to spiny 1 and 2 neurons, type 3 with aspiny 2, type 4 with aspiny 3, and types 5 and 6 with aspiny 1. Type 7 neurons are described below for the first time. A detailed description of the morphologic features of these types of neurons has been reported by Schmitt et al.[31]

The morphometric and stereologic techniques have been described by Haug.[15-17] In each putamen the neurons were evaluated within an area of 2,349,675 μm², which included 675 optical fields of 59×59 mm². Each neuron was measured planimetrically in the two dimensions of the microscopic projection plane (Figure 1). This was done by means of a magneto strictive table connected to a computer. On this table a mouse that generates an intense point of red light can be moved by the investigator. This point is projected via a mirror onto the microscopic projection plane. The investigator looks through the microscope and can see the point apparently in the plane of projection, where he can shift it around by moving the mouse. A computer program registers the movements of the mouse and calculates the values of the coordinates of the two-dimensional gravity centers, projection area, maximal diameter and form factor. The investigator has to assign each neuron to its appropriate type.

In addition to the first order stereology, further estimations with five different techniques were made in order to quantify various aspects of spatial distribution (second order stereology) of the seven types of neurons.

All structure analytical programs were devel-

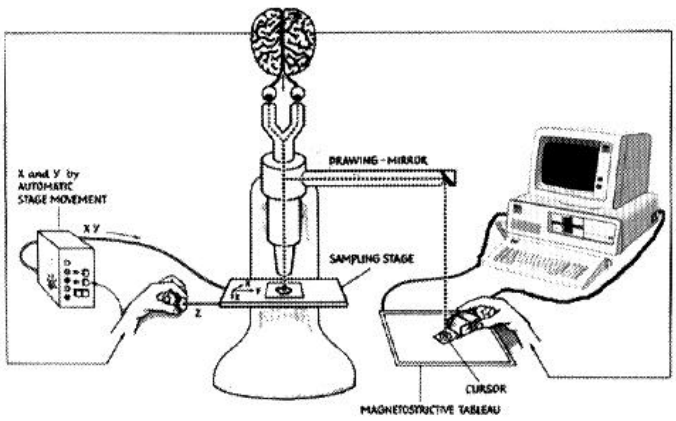

Figure 1 Setup of the measurement devices used for the morphometric evaluation of neurons in the human putamen.

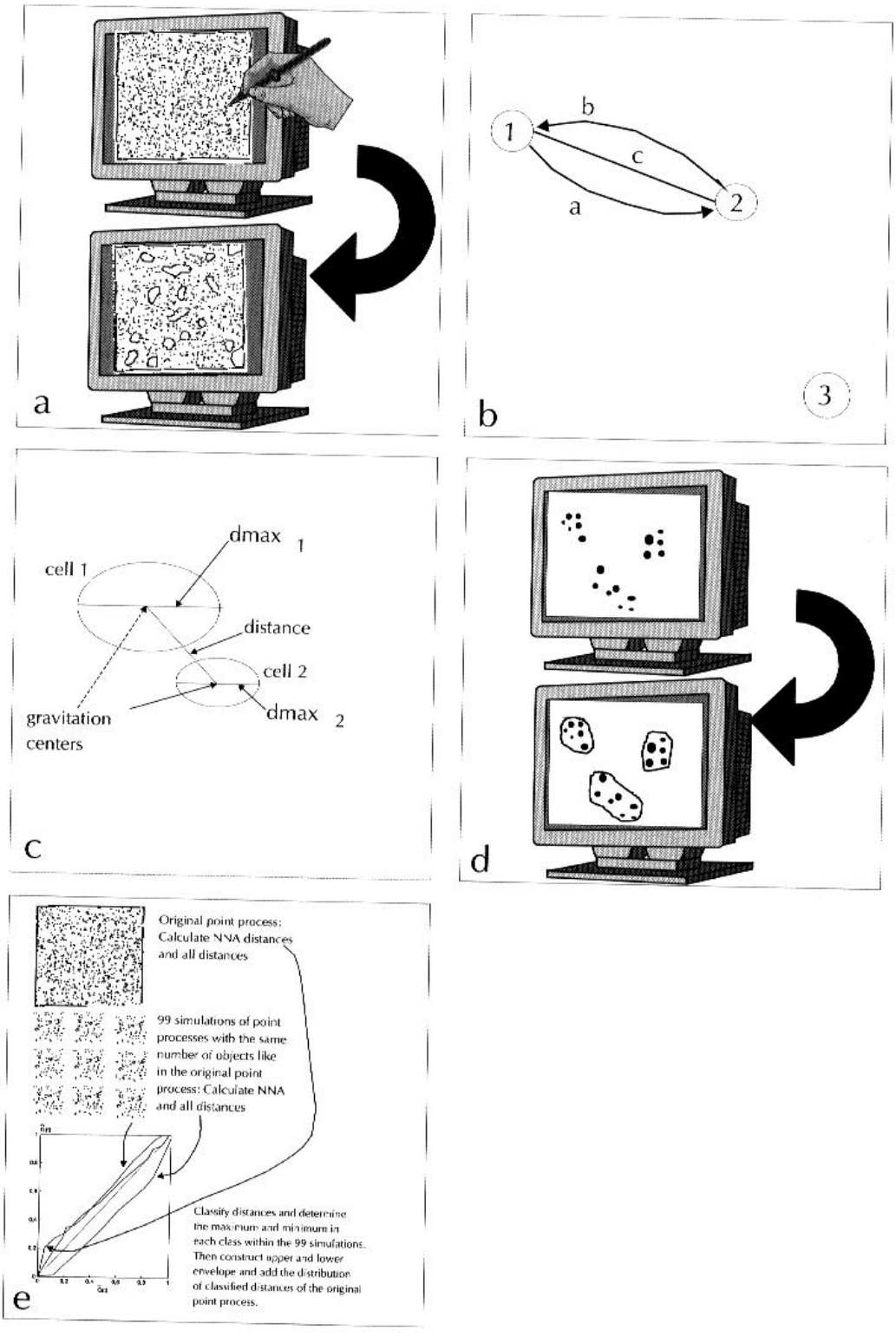

Figure 2 Overview of all the methods used in this work. (A) Visual point field analysis has to be carried out by a human investigator, supported by a computer that displays the gravitation centers of the neurons on a screen. Using a mouse, the investigator outlines distinct regions in the point field. (B) Display illustrating nearest neighborhood analysis: (a) computation of the cell nearest to cell 1, and (b) of the cell nearest to cell 2. (c) The distance between cells 1 and 2 is the same as that between cells 2 and 1. Cell 3 is not the nearest neighbor to either cell 1 or cell 2. (C) Sketch showing the factors used for stereologic cluster analysis. The mean of the maximal diameters of two different neurons and the distances to their gravitation centers are used to decide whether or not they ought to be connected. (D) Multivariate cluster analysis is used in order to classify neurons into groups, depending on their positions relative to one another. The result should be the formation of classes or groups. (E) Point process analysis is a statistical analysis of three different basic patterns (Figure 3) of distributed objects. The original point process has to be evaluated and simulations of virtual point processes for determination of the upper and lower envelope curves established. If the empirical distribution function derived from evaluation of the nonsimulated point field exceeds the upper or lower envelope, the point process is not random.

oped on ×86 computers (Intel). Only the multivariate cluster analysis (MCA) algorithms were written in C++; Pascal was used for the others (Figure 2).

Visual Point Field Analysis (VPA)

VPA is a method of defining by inspection the borders of areas within which neurons are distributed at an exceptionally high or low density. It is a useful technique if the complexity of the cytoarchitectonics increases to a point where the classification or segmentation of subregions becomes impossible by purely numerical methods. A point field is a distribution of objects (in this case, neurons) in a finite region or reference space. The principle of VPA was

worked out by Haug[14] and extended by Schmitt.[30] The gravitation centers of a certain type of neuron are plotted, for instance, on a computer screen. The investigator next outlines regions of high and low density; points are used to represent individual neurons. A new neuron population is then superimposed onto the first image and the regions compared. This is repeated for all possible types of neurons. If these regional patterns also appear in other putamina, they are considered to represent a regularly recurring arrangement.

Nearest Neighborhood Analysis (NNA)

NNA is a method introduced into the biological sciences by Clark and Evans.[6] It is based on the coordinates of the gravity centers of the various neuron types and depends upon systematic variation (equation 1) of the matrix indices containing the data records of the coordinates. This step is necessary because all pairs of coordinates must be combined in order to locate that neuron which is closest to the first, second, and so on, in the data list or matrix of the individual cells. For example, if one wishes to find the cell nearest a particular cell in focus, then the distances from all the surrounding cells have to be calculated. The shortest distance is then selected, and with this alone one can identify the required "closest cell." In order to find out which neuron is nearest another specified neuron, this systematic examination of variation in the distances between all the neurons is necessary. The result of such a variation involves two different neurons and calculation of their Euclidean distance, d, apart (equation 2). Equation 1 gives us the number of necessary combinations of coordinate pairs. It also shows how a systematic variation should be calculated and how many neurons (r) or other objects should be combined within one step.

$$A(\bar{V}) = \frac{K!}{(K-r)!}. \quad (1)$$

$A(\bar{V})$ = number of variations of gravity centers,
K = number of gravity centers of one population or a combination of populations, and
r = number of data sets (i.e., types of neurons) (in this case r = 2 because the distance between two neurons (pair of objects or of data sets (PDS)) is under consideration).

$$d(P_{x_i,y_i}; P_{x_j,y_j}) = \sqrt{(x_i - x_j)^2 + (y_i - y_j)^2}. \quad (2)$$

$d(P_i;P_j)$ = Euclidean distance between P_i and P_j, and
P = neuron with coordinates of the gravitation center at x and y.

$$A(\bar{v}) = K^r. \quad (3)$$

$A(\bar{v})$ = number of variations of types to PDS,
K = number of types (K = 7), and
r = number of PTN members (in this case r = 2 because PDS are considered).

Because different types of neurons must be taken into account, the combination strategy becomes more complex. This is because the types of neurons (PDS) have to be combined in the first step. For example, the nearest neighborhood distribution of type 1 neurons was analyzed first. The systematic variation (1) was therefore applied only to type 1 neurons (formally, this is described by $1 \rightarrow 1$). After this, the nearest neighborhood distances from neurons of type 1 to neurons of type 2 ($1 \rightarrow 2$) were calculated and the procedure extended.

The number of possible arrangements of the seven types of neurons into pairs of types was determined by using the combinatorial scheme already described. It can be calculated by means of equation 3.

In addition, higher PDS combinations were constructed and a chaining grammar formulated in order to quantify the type sequences and the algorithmic k-nearest neighborhood investigated. This means that the sum of the nearest neighborhood distances over a defined number of neurons (k) was determined. Such calculations are interesting because they provide information about the spatial distribution of the different types of neurons.

The calculation of nearest neighborhood distances was also employed in the point pattern analysis section. The difference between the method used here and that of point pattern analysis lies in the statistical analysis of the nearest neighborhood distances.

Stereologic Cluster Analysis (SCA)

Stereology provides methods of determining three-dimensional parameters from two-dimensional values. This kind of quantification, which is based on small samples, has many advantages over counting all the cells or structures of interest (sampling). *Cluster analysis* is a term derived from multivariate statistics. There are many different cluster analytical methods that may be used to detect statistically significant clusters or groups of data. These methods are of two kinds: (1) those which are able to collect single data points to form large clusters or groups, and (2) those which subdivide clusters that already exist.

The new term SCA combines the principles of both stereology and cluster analysis. The contribution of stereology to SCA lies in the fact that it employs such parameters as the maximal diameter of a cell or, in other words, additional morphometric parameters (size, roundness, etc., of biologic objects). The contribution of cluster analysis is that it offers a method by which groups of cells or neurons may be constructed. This involves calculation of the distances between certain objects and use of such criteria as maximal diameter.

Some types of neurons are situated so close together that under the light microscope their cytoplasm appears to be confluent. In order to find out if this apparent arrangement occurs in a random fashion and to what extent it differs between one population of neurons and another, it was necessary to develop a new technique, one that takes both the size of the neurons and their location into account. The largest diameters and the coordinates of the gravity centers of neurons could then be included in the subsequent calculations. SCA also makes use of a certain arrangement of the combinations, the number of cell combinations in the data record having been determined by equation 4. K is the number of neurons of a certain type that are necessary for performing the calculation described above, and r is the number of neurons to be combined in a single step of the calculation (in this case, two).

$$A(\bar{c}) = \frac{(K+r-1)!}{r!\,(K-1)!} \quad . \tag{4}$$

$A(\bar{c})$ = number of two-tuple combinations,
K = number of types of neurons (K = 7), and
r = number of PDS members (in this case r = 2 because we are working with PDS).

Before the calculation is started, PDS have to be assembled. All PDS combinations using equation 5 were investigated.

$$A(\overline{C}) = \frac{K!}{r!\,(K-r)!} \quad . \tag{5}$$

$A(\overline{C})$ = number of combinations of gravity centers,
K = number of gravity centers of one or combinations of populations, and
r = number of PDS members (in this case r = 2 because we are working with the distance between two neurons).

SCA was applied to each PDS combination in order to detect the different arrangements applying to the different types of neuron.

At the beginning of the calculation, all the neurons are unclassified—that is to say, no relationship between them has yet been determined. If a neuron is related to another neuron ("partner A") that is closest to it, then its partner A will be assigned to the first neuron, and an assignment is said to exist between them. In spite, however, of this assignment, only the first neuron is said to be classified. A new partner A must then be determined for the second neuron. This may well be the first neuron itself, but if it is a different neuron, then the original partner A can also be said to be classified. The process is then continued until all the neurons have been classified: the end of the classification procedure has been reached.

Now, taking the above example into account, a "chain" is generated by the algorithm, as follows. The first neuron having been assigned to the second one, a two-node chain can be said to exist. The second neuron is then assigned to a third one, and the three neurons, which are now interconnected by assignments, constitute what we describe as a "cluster." However, since an additional parameter (maximal diameter, obtained by measurement) can also be introduced into the calculation, the procedure may be adapted to more than two dimensions. We call this procedure *SCA*.

The assignment of unclassified neurons within the algorithm to other neurons, or to neurons that have already been classified, is controlled by the so-called *selection criterion* (C) of equation 7. C is the relationship between the size and distance of a PDS. If d (distance) is smaller than or equal to the sum of the two maximal radii (equation 6) of a PDS, then C is confirmed, and the PDS elements are classified as a new cluster. New, unclassified objects can naturally be added to existing clusters, and in this way the clusters will grow.

Up to now, the exact gravity center distance, d (neighborhood cluster analysis [NCA]), has been used. This means that neurons that are lying closer to each other than to more-distant neurons may be said to constitute a cluster. In order to select neurons that are (within a defined limit) "close together," C can be modified by a *distance factor*, f, by which d is multiplied in equation 8. If f is <1, C is valid only if the neurons are lying very close together (contact cluster analysis [CCA] f = 0.6). If, however, f is >1, neurons with larger distances are said to be connected.

$$D_{m(i,j)} = \frac{D_{m_i}}{2} + \frac{D_{m_j}}{2} \quad . \tag{6}$$

D_m = maximal diameter of a neuron.

$$f \times d\,(P_{x_i,y_i}; P_{x_j,y_j}) \leq D_{m(i,j)}. \quad (7)$$

$$d\,(P_{x_i,y_i}; P_{x_j,y_j}) \leq D_{m(i,j)}. \quad (8)$$

The distance factor can be considered a filter. If a small value is chosen, many neurons will not be selected, or "filtered out." It is also possible to follow the formation of clusters by increasing the distance factor stepwise (Table I).

MCA

Investigation of the spatial distribution of neurons by cluster analytical methods[19] was introduced following the results obtained by VPA. Different multivariate statistical algorithms were applied to the data sets in order to discover an algorithm capable of producing results comparable to those obtained by VPA. Enclosing clusters within a large, surrounding cluster might seem at first sight to be inconsistent. However, the methods were applied to each type of neuron separately, so that "cluster-overlapping A" or "cluster-embedding A" between different types of neurons could be taken into account.

In particular, the following procedures were employed: single linkage (nearest neighbor) (equation 9), complete linkage (farthest neighbor) (equation 10) and average linkage (equation 11) as hierarchic or agglomerative methods and the K-means (equation 12) as a partitioning technique. Single linkage starts at the finest partition of the data set. At this first step, each neuron is considered a cluster. Those neurons are then connected which are closest together. In equation 9 this process is expressed as a minimalization task. After this first clustering step, those clusters are connected which are nearest together and the procedure repeated until a certain number of clusters have been built up by the algorithm. The number of SCA clusters is equal to the number of clusters detected by VPA, the complete linkage method connecting only those that are farthest from each other. The distance between the clusters must therefore be maximized (equation 10). Another criterion for building clusters is defined within the average linkage. The average linkage method starts at a maximal partition of objects; that means that each neuron is considered a cluster. The algorithm then connects only those neurons lying at the smallest average distance apart. The final procedure starts from one large cluster of interconnected neurons, and the algorithm then halves this large cluster; this process is repeated further. Equation 12 lays down the procedure: until the number (k) of clusters is reached, search the data set (P) in all dimensions (J, here J = 2) for a partition that will produce the smallest distance between them. All algorithms continue to analyze the data sets until the target number of clusters defined by the investigator is reached. It is also possible, however, to define a criterion that should optimize the construction of clusters. The internal structure of the cluster is dependent upon the number of clusters that should be generated by a specific algorithm.[19]

Different kinds of distance measurement are tested by these methods. For NNA and SCA the Euclidean distance measurement (equation 2) is used. In order to explore the effects of some important distance measurements contained in the cluster analytical algorithms, the general formula for distance measurement is described.

The Minkowski q-metric (L_q-distances) (equation 13) is a general formula defining different metrics and distance measurements. A city block or chess board metric is given if q = 1 (equation 14). This simplest Minkowski metric is also called the L_1-norm. The next metric is the Euclidean metric (equation 2), or the L_2-norm. Finally, the Tschebyscheff metric (equation 15), or L_∞-norm, is applied.

$$d\,(P_{x_n,y_n}; P_{x_m,y_m}) \rightarrow \min_{n \neq m.} \quad (9)$$

$$d\,(P_{x_n,y_n}; P_{x_m,y_m}) \rightarrow \max_{n \neq m.} \quad (10)$$

$$d\,(K_n; K_m) = \frac{1}{K_N \times K_M} \sum_{n \in K_n}^{K_N} \sum_{m \in K_m}^{K_M} d_{nm} \rightarrow \min_{n \neq m} \quad (11)$$

K_n = class K_n,
K_m = class K_m,
K_N = number of elements in class K_n,
K_M = number of elements in class K_m, and
$d(K_n;_m)$ = mean distance between class K_n and class K_m.

Table I *Results of SCA with Different f*

f	$\bar{x}$n	$\bar{x}$c	$\bar{x}$s	$\bar{x}$f
2.0	246.0	2826.4	6.7	241.0
1.0	291.0	891.4	2.5	56.0
0.8	216.0	524.4	2.4	33.4
0.6	121.9	263.4	2.2	17.9

The mean number of connections ($\bar{x}$c) within a cluster is higher for f = 2 than the neuron number because one neuron can be connected to several others. The mean number of clusters ($\bar{x}$n), mean number of connections, mean cluster size ($\bar{x}$s) and mean frequency of cluster elements in relation to the whole population ($\bar{x}$f) decrease with decreasing f.

$$X(K) = \sum_{k=1}^{K} \sum_{p=1}^{P} \sum_{j=1}^{J} (P_{pj} - K_{kj}) \rightarrow \min. \quad (12)$$

X(K) = square of the deviation of the distance between P and K,
J = dimensions,
K = number of cluster centers, and
P = number of points or gravity centers.

$$d_q(P_n, P_m) = \left(\sum_{j=1}^{J} |P_{nj} - P_{mj}|^q\right)^{\frac{1}{q}}, \quad q \geq 1. \quad (13)$$

d = general Minkowski distance metric,
n, m = number of gravity centers,
P = point or gravity center (if J = 2: {x;y}, if J = 3: {x;y;z}), and
q = L-norm.

$$d_1(P_n; P_m) = \sum_{j=1}^{J} |P_{nj} - P_{mj}|. \quad (14)$$

$$d_\infty(P_n; P_m) = \sum_{j=1}^{J} \max\{|P_{nj} - P_{mj}|\}. \quad (15)$$

Point Pattern Analysis (PPA)

PPA is a method that analyzes point patterns in one or more dimensions statistically. An intuitive definition of a point pattern is the distribution of objects (in this case, neurons) distributed along a line or in a plane, space, and so on, according to the number of dimensions. In this study, continuous structures (i.e., neurons) were observed and then transformed into discrete structures in the data sets. In this case the transformation was determined by the measurement taken by the investigator. We are therefore using only the discrete formulas for the analysis of neuron organization.

The discrete objects can be points or symbols for cells. Point pattern analysis is used to detect structure in the spatial distribution of the neurons or points. This means that PPA is capable of analyzing a point distribution that is significantly different from a random distribution of the same number of points within the same reference space. The structure or pattern of points can be a clustering of objects, a distribution of points a certain distance apart (hard core) or a random process (Poisson process). A "process" is a distribution of "events" or objects within a particular dimensionality.

Two basic processes were employed here for the analysis of the distribution of neuron types. The global (H(t)) and nearest neighborhood (G(t)) tests of PPA were described in detail by Diggle.[7] Each test distinguishes between hard core processes, cluster processes (neurons spatially aggregated) and a Poisson process (equation 16). Such a Poisson process can be produced by a pseudorandomizing function (Monte Carlo simulation). If the neurons are distributed according to the Poisson distribution, the null hypothesis for so-called complete spatial randomness (CSR) is true.

$$P(n = k) = \frac{\lambda^k}{k!} e^{-\lambda}. \quad (16)$$

n = number of neurons, and
λ = mean of the distribution.

Because each type of neuron as well as certain combinations of neurons must be analyzed, a combinatorial scheme is again required. Therefore, the PDS was analyzed by using the combination scheme laid down by equation 5. These combinations of PDS and the calculation of their interevent distances, t_{ij}, (t_{ij} = dq (P_n, P_m) {q = 2}) (equation 13) result in their empirical distribution function (EDF), a concept introduced by Diggle. The EDF is based on distance calculations derived from measured objects or neurons ("empirical objects A") and not, for instance, from a theoretical distribution, such as that of equation 16. The distances between neurons (or interevent distances) are calculated within a further combination of data points in the algorithm. This analysis can therefore be regarded as a hierarchic combination of data points within a combination of neuron types. EDF is normalized between 0 and 1 by equation 17 for $\bar{H}(t)$ and by equation 18 for $\bar{G}(t)$. $\bar{H}(t)$is calculated for all the distances between neurons, whereas $\bar{G}(t)$ determines the nearest neighborhood distances, t_i. In addition, 99 simulations were performed in order to generate 99 Poisson point processes. These Poisson distributions consist of the same number of points as in the distribution that was not simulated, and the coordinate maxima and minima (reference space) are also the same.

The H(t) and G(t) algorithms are then used to analyze these simulated distributions. Each calculated t_i is assigned to a 5-µm-wide class (number of classes, 128). If, for example, two neurons were to have a distance apart of 18 µm, these distances would be assigned to class 4, and two new results would be entered that were new to this class. After these interevent distances were classified, the maximum and minimum frequency of each class within 99 simulations was determined. Based on these maxima and minima frequencies of the analyzed random point processes, the so-called upper (U(t)) and

lower simulation envelopes (L(t)) were calculated. The upper simulation envelope represents the maxima of frequencies within 99 simulations, whereas the lower simulation envelope shows the minima of the frequencies. This kind of presentation of the limits of a random distribution has the advantage that one requires only one diagram in order to decide whether a certain interevent distance is not random, meaning that it lies outside the envelope. EDF, U(t) and L(t) are plotted in one diagram (Figure 3). If EDF exceeds U(t), a significant ($P \leq .01$) cluster process is detected, and if EDF falls below

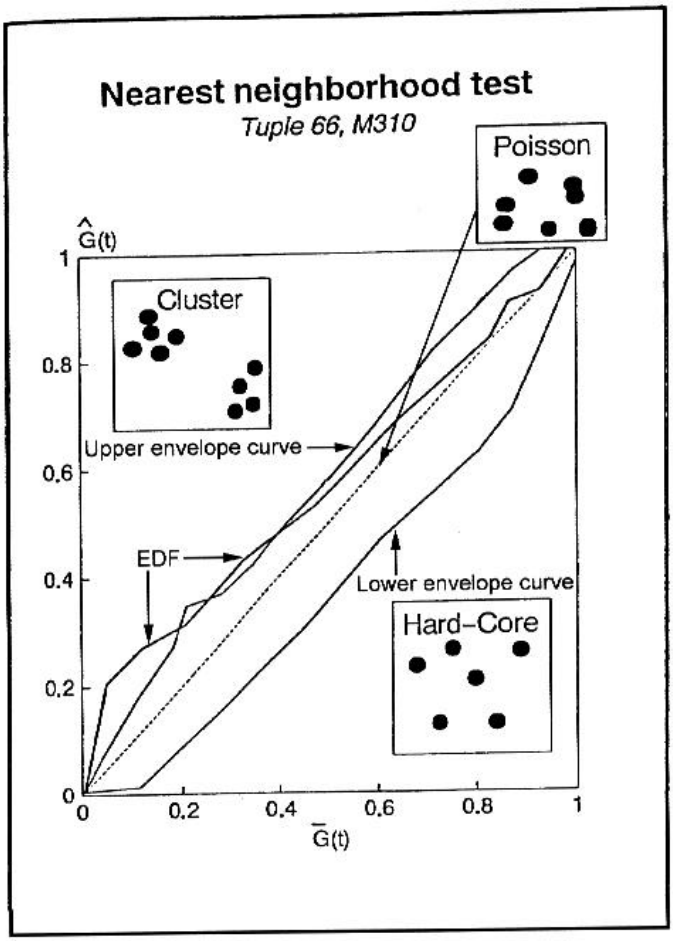

Figure 3 Result of a point process analysis of PDS 6→6 of one human putamen using the nearest neighborhood method. The typical arrangements of three point processes are shown in the boxes. The abscissa represents the normalized distances and the ordinate the normalized frequencies. The diagonal curve (G(t)) (broken line) reveals a Poisson distribution surrounded by the curve of the upper envelope. This is very steep, about 0.2 ($\bar{G}(t)$), and lies above the G(t) curve and the curve of the lower envelope, which is very flat, about 0.2 ($\bar{G}(t)$), and that lies below the G(t) curve. The EDF curve lies above the upper envelope curve (between 0 and 0.2 or 0.3 and 0.4 $\bar{G}(t)$). This means that the distribution for small distances differs significantly from a random distribution.

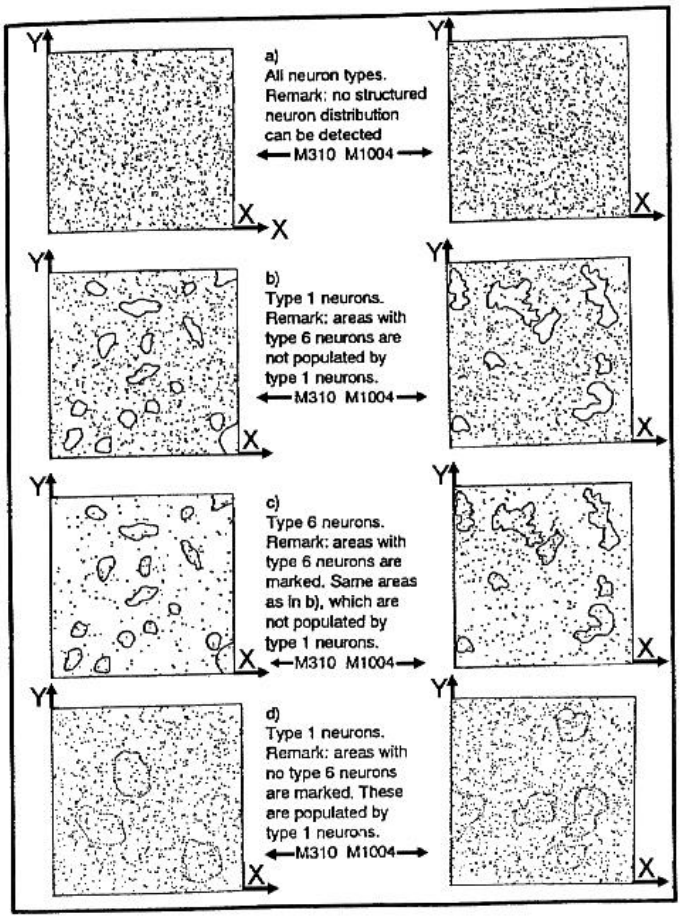

Figure 4 Graphic representation of a VPA in the human putamen. In order to make the picture clearer, the x-scale is 2.5 times greater than the y-scale (indicated by the two arrows at the top right diagram). The outlines were produced by a drawing involving the comparison of each of the neuron populations.

L(t), a significant hard core process is detected. If EDF takes its course within the limits of U(t) and L(t), then the point process is Poisson distributed, and a CSR exists.

$$\overline{H}(t) = \left(\frac{n(n-1)}{2}\right)^{-1} N(t_{ij} \leq t). \tag{17}$$

$N(t_{ij} \leq t)$ = number of distances.

$$\overline{G}(t) = n^{-1}\, N(t_i \leq t). \tag{18}$$

$N(t_i \leq t)$ = number of nearest neighborhood distances.

In order to obviate a biased calculation, not all neurons lying close to the evaluation border were used. If their distance to the border was smaller than their maximal diameter, they were rejected.[34]

Results

VPA

VPA shows clear inhomogeneity of the spatial dis-

Table II *Mean Nearest Neighborhood Distances of All Variations of PDS in the Human Putamen*

	PDS element (μm)						
Type	**1**	**2**	**3**	**4**	**5**	**6**	**7**
1	20	138	413	268	86	32	374
2	22	139	409	275	92	33	373
3	22	129	268	256	118	32	500
4	23	146	418	451	94	31	390
5	18	135	435	266	78	34	369
6	20	139	416	269	89	28	376
7	27	209	609	378	123	43	395

The distances between the PDS element 1 and other types in the first column are small because this population has the highest density.

tribution of the different types of neurons. In Figure 4, VPA was applied to two different putamina. One column with four images is shown on the left and the other on the right.

In Figure 4, regions with high densities of type 6 neurons and no (or only a few) type 1 neurons are interactively outlined. In regions that include type 1 neurons, no (or only a few) type 6 neurons were found. Some regions containing certain types of neurons are clearly separated, whereas others partly overlap.

NNA

An NNA plot is represented in Figure 5A and B. Table II summarizes the mean distances between all variations of types of neurons. Significant differences ($P \leq .05$) between the original distribution and Monte Carlo simulations were found for PDS to be $2 \rightarrow 1$, $4 \rightarrow 1$, $5 \rightarrow 5$, $6 \rightarrow 2$ (Dixon Mood test) and $4 \rightarrow 1$, $4 \rightarrow 6$, $6 \rightarrow 1$ (Kolmogoroff-Smirnoff test). The mean distances were smaller if one PDS member had high spatial density (e.g., type 1 or 6). The mean distances of the different types of neurons are summarized in Table II. The mean distance of PDS $4 \rightarrow 1$ differs from PDS $1 \rightarrow 4$ because many neurons of type 1 that are positioned close to one type 4 neuron possess higher mean nearest distance than the same type 4 neuron to its closest type 1 neuron.

Because there are many more neurons in population 1, the mean distance from a type 4 neuron to the closest neuron of population 1 is small (PDS $4 \rightarrow 1$: 23 μm). Starting with a data set of type 1 neurons, it was possible to identify by calculation the nearest neurons of type 4. Because many type 1 neurons must be assigned to a few (sometimes distant) type 4 neurons, the mean nearest neighborhood distance increases.

SCA

A plot of NCA with f = 1.0 is shown in Figure 5C and D. Some neurons are not connected because they do not fulfill C. The results of the estimations are shown in Tables I, III and IV. The statistical hy-

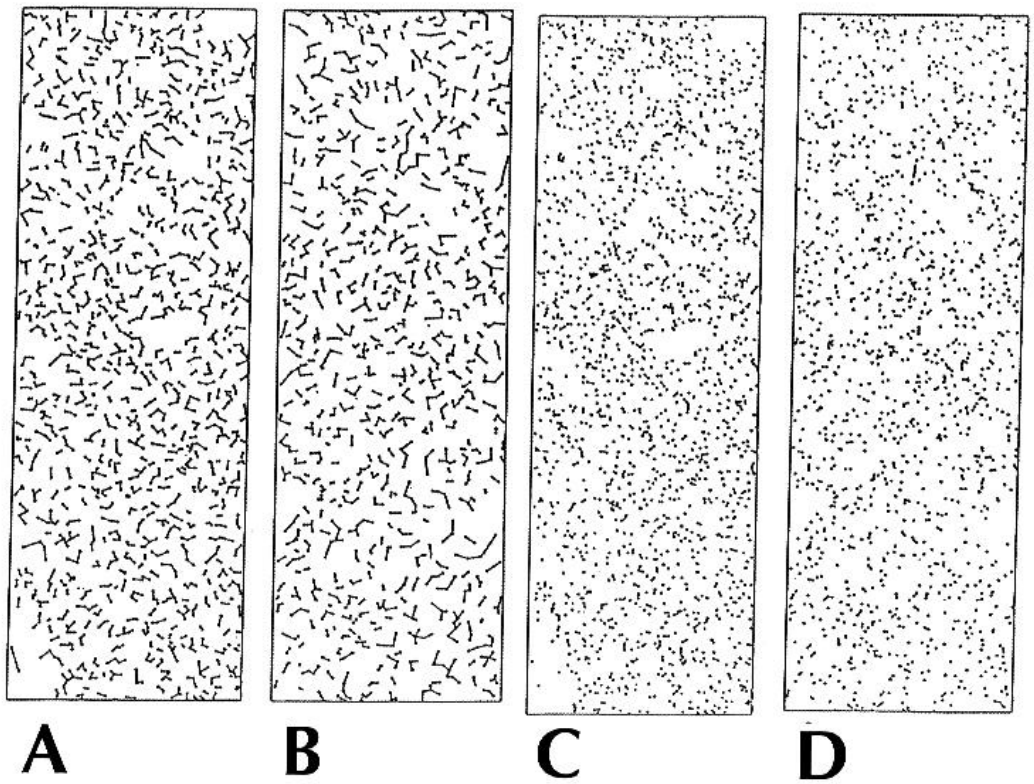

Figure 5 (A) NNA plot of all types of neurons in the putamen from a 25-year-old individual and (B) from a 100-year-old individual. (C) For comparison, the results of an NCA of all types of neurons in the putamen from a 25-year-old individual and (D) a 100-year-old individual are shown. The x- and y-scales are the same.

Table III *Dependence of Ratios of Mean Normalized Cluster Size Frequencies on Variations of f*

f	Mode	CR = 2	CR = 3	CR = 4
2.0	OD	3	2	1
	RC	3	1	1
1.0	OD	10	3	1
	RC	9	3	1
0.8	OD	21	4	1
	RC	12	3	1
0.6	OD	45	5	1
	RC	35	5	1

CR = cluster size ratio, OD = original data, RC = randomized coordinates of gravitation centers.

pothesis of a nonrandom clustering of neurons was tested using the U test. The mean distances of neurons building a cluster were compared with the randomized positionings of the types of neurons. The neurons of types 1 and 5–7 are not randomly distributed (U test, $P \leq .01$). Furthermore, a systematic modification of the simulation parameters (coordinates, maximal diameters) was carried out. This gave the following result: the mean distances between cluster members (Table IV, D) increase with the increase in the number of randomized variables (compare Table IV, f = 1.0). If f is increased to 4.0, then each neuron will be connected. If it is reduced to 0.3, only one small cluster will be calculated. These values must be characteristic features of the neuron population in the human putamen because they were similar in all 27 brains examined.

MCA

Different cluster analytical procedures were applied to the data in order to compare the results of MCA and VPA and to find out if there exists an automated procedure that produces results comparable to those of VPA. The algorithms of MCA show considerable differences in their cluster formations. The results do not show any similarities to those obtained with VPA (Figure 4). The well-known phenomenon of chain building from those of the single linkage algorithm results in both extremely long chains (Figure 6A) and extremely small clusters (Figure 6B–D). In Figure 6A, four clusters are depicted: three small ones (outlined near the upper border of the diagram) and a large, massively connected chain, which is not outlined.

In order to compare the results of the different distance measurements, the single linkage (Figure 6A–D) and K-means diagrams (Figure 6E and G) are represented. The diagrams have all the same scale. Each distance measurement leads to another cluster formation. This leads to the particularly elongated cluster structure shown in Figure 6F. These results suggest that it is inadvisable to use a standard algorithm with an arbitrary distance measurement instead of the design of a cluster analysis adapted to the problem or pattern. This means that the results of VPA cannot be generated by an MCA technique and that VPA cannot be replaced by MCA.

Point Pattern Analysis

This method provides a concise statistical analysis of the different neuron type assemblies or PDS, including all seven types. The thick line of the small neuron PDS $6 \rightarrow 6$ crosses the curve of the upper simulation function (Figure 3). This means that the clusters consist of closely situated type 6 neurons. Furthermore, this process is significant ($P \leq .05$) and is in accordance with the visual impression. The PDS $1 \rightarrow 1$ between the most frequent type 1 shows, in the near distances within the G(t) empirical distribution function, a significant hard core process. This means that the distances from cells of this type to other cells of the same type are greater than predicted by a completely random spatial distribution.

Application of all the structural analytical techniques was examined for any possible relationship to the age of the subject. The principal placement of

Table IV *Mean Results of SCA with Different Values of f and Randomization Modes*

f	OD D	OD C	OD C/t	RC D	RC C	RC C/t	RD D	RD C	RD C/t	RDC D	RDC C	RDC C/t
0.6	7.44	16.77	0.92	7.53	17.76	0.97	—	—	—	—	—	—
0.8	10.04	17.06	0.94	12.36	19.80	1.08	—	—	—	—	—	—
1.0	12.69	17.20	0.94	13.07	17.60	0.95	14.47	19.53	1.07	16.02	19.62	1.07
2.0	25.57	17.09	0.94	40.66	17.17	0.94	—	—	—	—	—	—

OD = original data, RC = randomized coordinates, RD = randomized diameters, RDC = randomized coordinates and diameters, D = mean Euclidean distance (μm), C = mean diameter of connected neurons, C/t = quotient of C and section thickness.

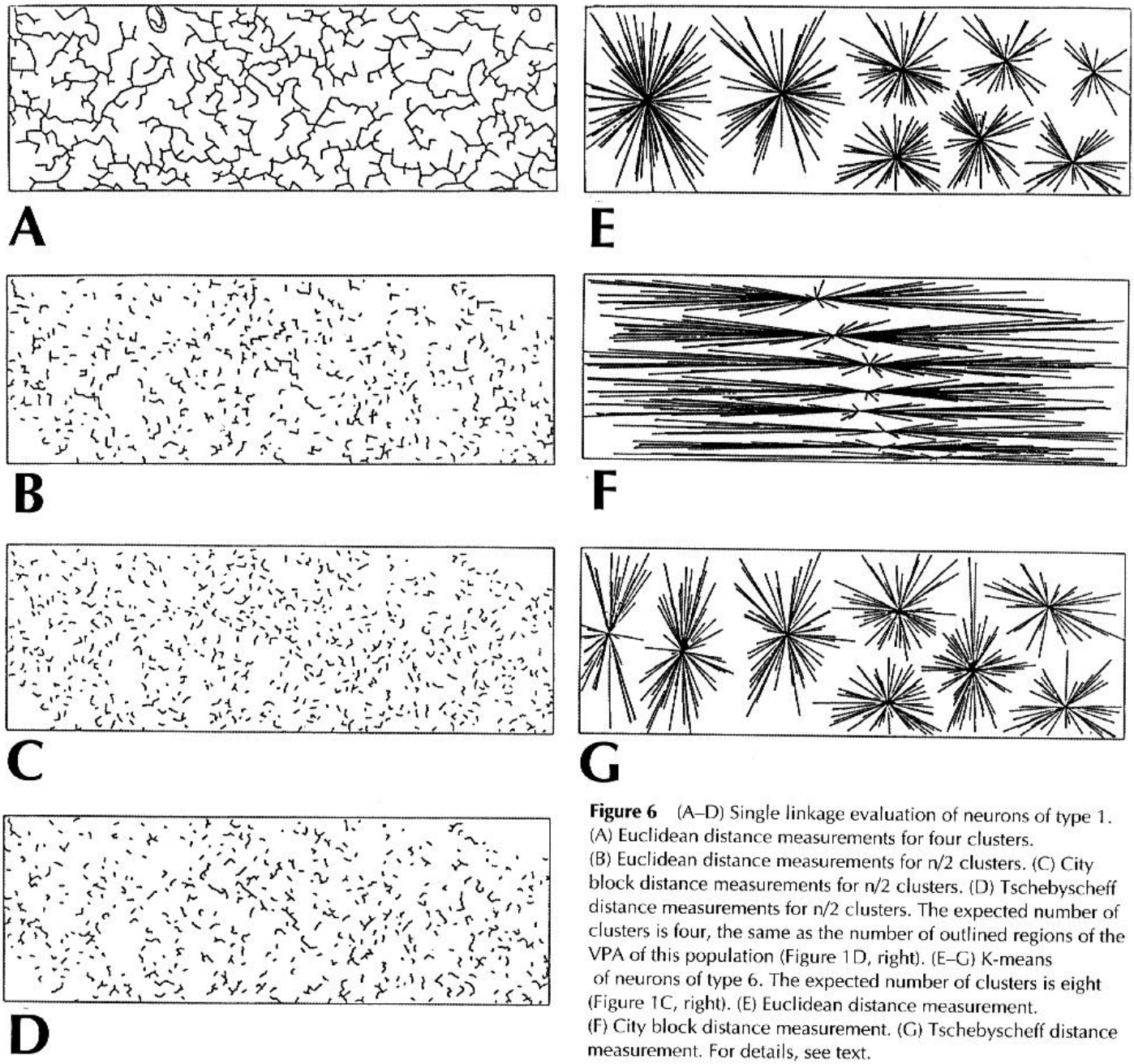

Figure 6 (A–D) Single linkage evaluation of neurons of type 1. (A) Euclidean distance measurements for four clusters. (B) Euclidean distance measurements for n/2 clusters. (C) City block distance measurements for n/2 clusters. (D) Tschebyscheff distance measurements for n/2 clusters. The expected number of clusters is four, the same as the number of outlined regions of the VPA of this population (Figure 1D, right). (E–G) K-means of neurons of type 6. The expected number of clusters is eight (Figure 1C, right). (E) Euclidean distance measurement. (F) City block distance measurement. (G) Tschebyscheff distance measurement. For details, see text.

neurons in the human putamen does not change with aging. Nevertheless, because of the normal shrinkage of the human brain with advancing age, the neurons in the putamen draw closer together as the subject gets older.

Discussion

With the aid of structure analytical methods, a significant cluster process of type 6 neurons and a significant hard core process (the neurons distributed at certain distances) of type 1 neurons could be revealed. NNA and SCA confirm these results. The VPA is useful for the recognition of fuzzy point patterns, the points of which overlap. So far, no procedure of MCA has been found that can replace VPA or that allows detection of those arrangements that are close to the VPA results. It is clear that type 6 neurons forming clusters surrounded by type 1 areas will not be distinguished as a single cluster. However, the MCA techniques used here are being applied for the first time to just such data sets. We searched regions similar to those generated by VPA

as well as new structural arrangements of the whole neuronal population.

In this study, two-dimensional neuron distributions were investigated. Further evaluations will be undertaken in order to extend the analysis to three dimensions and to compare smaller, three-dimensional section volumes with the large, two-dimensional section surface presented here.

So far it has not been clear whether a certain arrangement of neuron types can be correlated with the function of that pattern or if there is wavefront processing of biosignals in the local circuits or in regionally distributed neuron clusters. Nevertheless, even from the physical point of view, it seems likely that the time lapses between juxtapositioned neurons are shorter than between neurons located at a greater distance. Furthermore, it seems evident that the signal transfer time over short distances is lower than over longer distances. However, it is not known whether the myelination pattern of the axons and the neurophysiologic features of dendrites are the same for all the different spatially distributed populations, and it is also true that certain differences in the synapses can delay signal transduction and influence signal processing in a spatial arrangement of neurons.

This aspect of the packing and distribution of neurons in a network was considered by Young[38] and, more recently, by van Essen[36] as well as by Singer.[32] However, they took into account only the connectivity and neurogenetic features of neuronal networks.

It is necessary to learn more about the morphology (silver impregnation and neurotransmitter immunohistochemistry) of the types of neurons differentiated by AFC staining and about their neurophysiologic features. However, the possibility that their distribution or structure may influence neuronal function should be kept in mind.

Additional methods, such as tesselation analysis and pair correlation function,[26,34] are necessary to describe the arrangement of neurons, not only in the putamen, but also as a fundamental part of the comparative studies of the spatial pattern of the cerebral cortex in humans and other species by structure analysis. The anisotropy of neurons in the laminar and columnar regions of the cortex can be analyzed by laminar-specific NNA. The columnar regions involve highly anisotropic neuron distributions that can be quantified by texture analysis for periodicity[10] and orientation analysis.[34] With regard to Brodmann's area 33 in the cingulate gyrus, additional problems arise because the degree of lamination decreases here from six layers to a small band of neurons. The hippocampal formation includes the highly variable distribution and lamination of different kinds of neurons. There is, apart from a decrease in the number of laminars, a regular formation of clustered neurons in the entorhinal region. Structure analytical methods should be selected and applied to typical spatial arrangements of the structures of interest—i.e., neurons and glial cells. They are useful tools for detecting highly complex distributions of neurons within the brain that cannot be recognized by simple visual inspection. Furthermore, such techniques can be useful for the description and analysis of pathologic cell distribution. For example, they can be employed for the identification of malignant tissue.[24,25]

Finally, structure analytical methods can be applied to the postmortem brains of patients who have suffered from certain neurologic diseases and also for research in developmental neurobiology.

References

1. Baader SL, Baader KL, Schilling K: Software implementation of statistical methods for the analysis of structure and patterns in neuroanatomical objects. Brain Res Prot 1998;3: 173–182
2. Benes FM, Matthysse SW, Davidson J, Bird ED: The spatial distribution of neurons and glia in human cortex based on the Poisson distribution. Analyt Quant Cytol Histol 1987;9: 531–534
3. Böttcher J: Morphology of the basal ganglia in Parkinson disease. Acta Neurol Scand (suppl) 1975;52:7–87
4. Braak H, Braak E: Neuronal types in the striatum of man. Cell Tissue Res 1982;227:319–342
5. Braendgaard H, Gundersen HJG: The impact of recent stereological advances on quantitative studies of the nervous system. J Neurosci Meth 1986;18:39–78
6. Clark PJ, Evans FC: Distance to nearest neighbour as a measure of spatial relationships in populations. Ecology 1954;35: 445–453
7. Diggle PJ: Statistical Analysis of Spatial Point Patterns. London, Academic Press, 1983, pp 10–23
8. Foix C, Nicolesco J: Les noyaux gris centraux et la région mésencéphalosous-optique. Paris, Masson, 1925, pp 296–298
9. Fox CA, Andrade AN, Hillman DE, Schwyn RC: The spiny neurons in the primate striatum: A Golgi and electron microscopic study. J Hirnforsch 1971;13:181–201
10. Gonzalez RC, Woods RE: Digital Image Processing. Reading, Pennsylvania, Addison-Wesley, 1993, pp 506–518
11. Graveland GA, Williams RS, Difiglia MA: Golgi study of the human neostriatum: Neurons and afferent fibers. J Comp Neurol 1985;234:317–333
12. Graybiel AM, Ragsdale CW: Histochemically distinct com-

partments in the striatum of human, monkey and cat demonstrated by acetylcholinesterase staining. Proc Natl Acad Sci USA 1978;75:5723–5726

13. Hatten ME, Heintz N: Mechanisms of neural patterning and specification in the developing cerebellum. Annu Rev Neurosci 1995;18:385–408
14. Haug H: Clustering and layering of neurons in the central nervous system. Lecture Notes Biomath 1978;23:193–201
15. Haug H: Macroscopic and microscopic morphometry of the human brain and cortex: A survey in the light of new results. Brain Pathol 1984;1:123–149
16. Haug H: Stereological methods in the analysis of neuronal parameters in the central nervous system. J Microsc 1972;95: 165–180
17. Haug H: The evaluation of cell-densities and of nerve-cell-size distribution by stereological procedures in a layered tissue (cortex cerebri). Microsc Acta 1979;82:147–161
18. Holt DJ, Graybiel AM, Saper CB: Neurochemical architecture of the human striatum. J Comp Neurol 1997;384:1–25
19. Jain AK, Dubes RC: Algorithms for Clustering Data. Englewood Cliffs, New Jersey, Prentice-Hall, 1988 pp 58–133
20. Kemp JM: An electron microscopic study of the termination of afferent fibers in the caudate nucleus. Brain Res 1968;11: 464–467
21. Kemp JM, Powell TPS: The structure of the caudate nucleus of cat: Light and electron microscopy. Philos Trans R Soc Lond Biol 1971;262:383–401
22. Lu EJ, Brown WJ: The developing caudate nucleus in the euthyroid and hypothyroid rat. J Comp Neurol 1977;171: 261–284
23. Mariani AP, Kolb H, Nelson R: Dopamine-containing amacrine cells of rhesus monkey retina parallel rods in spatial distribution. Brain Res 1984;322:1–7
24. Mattfeld T: Nonlinear deterministic analysis of tissue texture: A stereological study on mastopathic and mammary cancer tissue using chaos theory. J Microsc 1996;185:47–66
25. Mattfeld T, Frey H, Rose C: Second-order stereology of benign and malignant alteration of the human mammary gland. J Microsc 1992;171:143–151
26. Okabe A, Boots B, Sugihara K: Spatial tesselations concepts and applications of Voronoi diagrams. New York, John Wiley & Sons, 1992, pp 405–432
27. Ranke T-P, Ranke I, Schwandtke A, Rother P: Quantitative Analyse von Chondrocytenverteilungsmustern im hyalinen Knorpelgewebe-Vergleich verschiedener Modelle. Gegenbaurs Morphol Jahrb 1989;135:125–131
28. Rother P, Stoyan D, Ranke T-P, Ranke I, Kreutz W: Quantitative Analyse des Chondrocytenverteilungsmusters im transitorischen hyalinen Knorpel der embryonalen Anlage von Sternum und Patella. Z Mikrosk Anat Forsch 1987;101: 69–78
29. Ruiz I, Altaba A: Pattern formation in the vertebrate neural plate. Trends Neurosci 1994;17:233–247
30. Schmitt O: Die Cytoarchitektonik des menschlichen Putamen: Eine qualitative und quantitative Typisierung der Neuronen, ihre Altersveränderungen sowie Analyse zweidimensionaler Verteilungen. Medical thesis, University of Lübeck, 1991
31. Schmitt O, Eggers R, Haug H: Quantitative investigations into the histostructural nature of the human putamen: I. Staining, cell classification and morphometry. Ann Anat 1995;177:243–250
32. Singer W: Funktionelle Organisation der Großhirnrinde. Naturwiss Rundschau 1997;50:386–394
33. Spiegel E: Die Kerne im Vorderhirn der Säuger. Arb Neurol Inst Wien Uni 1919;22:418–497
34. Stoyan D, Stoyan H: Fraktale Formen Punktfelder. Berlin, Akademie Verlag, 1992
35. Tennyson VM, Marco LA: Intrinsic connections of caudate neurons: II. Fluorescence and electron microscopy following chronic isolation. Brain Res 1973;53:307–317
36. Van Essen DC: A tension-based theory of morphologenesis and compact wiring in the central nervous system. Nature 1997;285:313–318
37. Vogt C, Vogt O: Zur Lehre der Erkrankungen des striären Systems. J Psychol Neurol 1920;25:651–655
38. Young MP, Scannel JW, Burns G: The analysis of cortical connectivity. Heidelberg, Springer, 1995